

Analyses of How the Design of a Hybrid Performance Stabilization System Affects Spinal Motion and Intervertebral Disc Pressure Using Finite Element Method

Chia-Wen Lee,^{1,2} Hao-Yuan Hsiao,³ Chao-Ming Hsu,³
Chih-Kun Hsiao,^{4*} Qiang Wang,^{1,2} and Cheng-Fu Yang^{5,6**}

¹School of Information Engineering, Xiamen Ocean Vocational College, Xiamen 361102, China

²Marine Culture & Tourism Integration of Fujian Higher Educational Applied Liberal Arts Research Center, Xiamen 361102, China

³Department of Mechanical Engineering, National Kaohsiung University of Science and Technology, Kaohsiung 807, Taiwan

⁴Department of Orthopedics, E-Da Hospital, I-Shou University, Kaohsiung 824, Taiwan

⁵Department of Chemical and Materials Engineering, National University of Kaohsiung, Kaohsiung 811, Taiwan

⁶Department of Aeronautical Engineering, Chaoyang University of Technology, Taichung 413, Taiwan

(Received January 27, 2025; accepted April 17, 2025)

Keywords: hybrid performance stabilization system, computed tomography, Mimics software, Solidworks software, ANSYS software

The hybrid performance stabilization (HPS) system combines rods, transitional screws, and coupler designs to provide semirigid fixation. This system maintains some range of motion near the fusion site during spinal fusion surgery, which may reduce compensatory effects at adjacent vertebral segments. However, clinical reports have shown the early degeneration of adjacent segments even in nonfusion surgeries, indicating that further research is needed on both the HPS design and its clinical applications. In this study, we began by collecting computed tomography (CT) scanning images from the twelfth thoracic vertebra (T12) to the first sacral vertebra (S1). Using Mimics software, vertebral contours were traced from these CT slices to create geometric models. The HPS coupler was then modeled using Solidworks software. Both models were subsequently meshed to create finite element models for analysis using ANSYS software. In this research, we investigated how varying the stiffness of the HPS coupler affected vertebral segment mobility and disc stress under flexion, extension, and lateral bending conditions. Additionally, we examined the suitability of HPS for intervertebral discs with moderate to severe degeneration by simulating these degenerative conditions.

1. Introduction

The spine, consisting of thirty-three vertebrae, serves as the primary supporting structure of the human body. Its essential functions include protecting the spinal cord, supporting body weight, and facilitating load transfer during physical movement. Below the cervical spine are

*Corresponding author: e-mail: ed108805@edah.org.tw

**Corresponding author: e-mail: cfyang@nuk.edu.tw

<https://doi.org/10.18494/SAM5568>

twelve thoracic vertebrae, which connect to the ribs to protect vital organs such as the heart and lungs. The lumbar spine, comprising five vertebrae in the lower back, experiences significantly higher loads than other spinal segments, resulting in a considerably higher incidence of pathological conditions in this region.⁽¹⁾ The lumbar spine is particularly susceptible to pathological changes among all spinal segments owing to its extensive range of motion and the substantial mechanical loads it bears. Poor posture maintained over extended periods and excessive strain from lifting heavy objects can lead to various lumbar spine disorders. Common lumbar spine conditions include spondylolisthesis, spinal stenosis, herniation of intervertebral discs, and degenerative disc disease. These conditions often develop as a result of the unique biomechanical demands placed on the lumbar region during daily activities and the natural aging process.

The relationship between dynamic spinal stabilization system design parameters and sensor integration represents a crucial advancement in modern spine treatment technology.⁽²⁻⁴⁾ The fundamental purpose of these systems is to provide adequate spinal support while maintaining vertebral flexibility. The system's design incorporates sophisticated engineering principles that balance mechanical support with natural movement patterns, ensuring optimal load distribution and force transmission throughout the spinal column. The integration of sensors within hybrid performance stabilization (HPS) systems plays a vital role in monitoring spinal conditions in real time, providing crucial feedback for system operation and adjustment.⁽⁵⁻⁷⁾ These sensors enable the continuous assessment of various biomechanical parameters, including load distribution, motion patterns, and positional changes. Through advanced sensing technologies, the system can monitor spinal alignment and make real-time adjustments to maintain optimal therapeutic conditions. This capability is further enhanced by the incorporation of wearable sensors that provide continuous monitoring capabilities. The system's ability to monitor loads and forces ensures that mechanical support remains within therapeutic ranges while maintaining spinal flexibility.

Motion and position sensing capabilities allow for the precise tracking of spinal movement patterns, enabling treatment strategies that are more effective than traditional methods. The real-time feedback mechanisms facilitate immediate adjustments to optimize therapeutic outcomes, while alignment monitoring ensures appropriate spinal positioning throughout movement. This integration of wearable sensors with monitoring capabilities represents a significant advancement in personalized spine care, allowing for more precise and adaptable treatment approaches. However, the complexity and challenges inherent in HPS system design necessitate advanced simulation capabilities for effective development and optimization. The implementation of simulation systems for preliminary result prediction can significantly reduce design time and enhance design efficiency.

The finite element method (FEM) stands as one of the most powerful numerical analysis techniques available, particularly adept at solving problems involving complex geometric shapes and boundary conditions.⁽⁸⁾ In recent years, the adoption of FEM in biomedical applications has been driven by several practical limitations in conventional research approaches, including limited availability, high costs, and inherent difficulties in conducting repeated trials. Moreover, traditional experimental methods often struggle to provide detailed insights into internal

biomechanical behaviors of biological systems. These limitations have positioned FEM as an invaluable analytical tool in the field. FEM offers distinct advantages in biomechanical analysis through its ability to simulate various scenarios by adjusting parameters systematically. This approach provides reproducible results at a relatively low cost, enabling researchers to develop a deeper understanding of biomechanical behaviors under different conditions. The method's flexibility allows for the comprehensive investigation of multiple variables and their interactions, which would be extremely difficult or impossible to achieve through physical experimentation alone.

In this study, we aim to investigate the biomechanical characteristics of the posterior HPS from both FEM and biomechanical perspectives.^(9,10) On the basis of the operational mechanism of the dynamic stabilization system, the design parameters of the system's coupler will be altered. Moreover, we will explore the effects of different coupler stiffnesses on vertebral motion and intervertebral disc pressure (interdisc pressure) under conditions of flexion, extension, and lateral bending. The goal is to use the results of the finite element analysis to understand the applicability of the HPS for intervertebral discs at varying stages of degeneration, and to assess the anticipated functional changes when design parameters are modified. Ultimately, we aim to provide valuable insights for the improvement of existing products or the development of new implants by offering design references. However, it is crucial to recognize that FEM is not a complete solution in itself, but rather an analytical tool that provides valuable insights and directions for investigation. Although it can generate important clues and suggest potential solutions, these findings should be interpreted as guidance for further investigation rather than definitive answers. The method's results serve as valuable indicators of decision-making and direct subsequent research efforts while still requiring validation through other means when possible.

2. Methodology

In this research, we utilized human cadaveric spine specimens spanning from the twelfth thoracic vertebra to the sacrum (T12 to sacrum). We acquired twelve normal spinal specimens without spinal injuries or pathologies from the Anatomic Gift Registry (AGR), with appropriate authorization from the institution for research purposes. Prior to experimentation, each spinal specimen underwent bone density assessment using either dual-energy X-ray absorptiometry or computed tomography (CT) scanning. During scanning, a calibration phantom with known density was placed alongside the specimens to enable a comparative image analysis for determining bone density. After obtaining bone density data for all specimens, statistical methods were employed to divide them into three groups of four spines each. The grouping was carefully adjusted to ensure that no statistically significant difference in bone density existed between groups, thereby minimizing potential experimental errors stemming from varying bone density levels among specimens. The commercial software Materialize Mimics was employed to segment vertebral bodies from CT scan slices and create three-dimensional models from the twelfth thoracic vertebra (T12) to the first sacral vertebra (S1), as illustrated in Figs. 1(a) and 1(b).

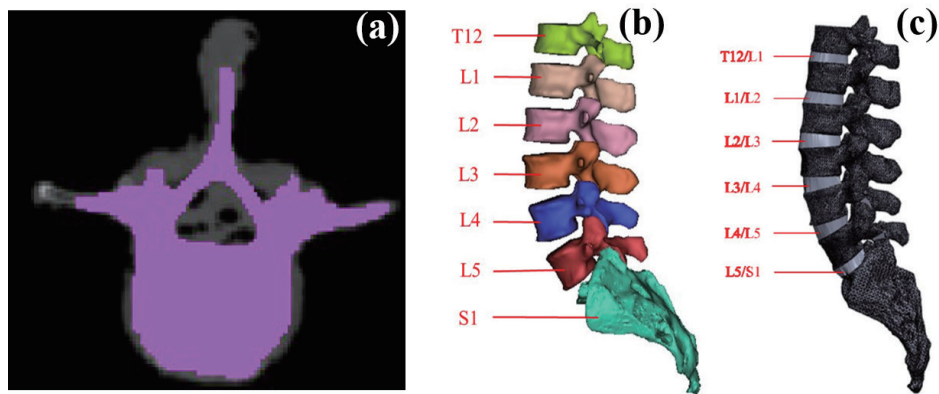


Fig. 1. (Color online) (a) Selection of vertebrae in Mimics software after CT scanning, (b) spinal model created in Mimics software, and (c) intervertebral disc created in Solidworks software.

Individual stereolithography (STL) files were generated for each vertebral segment. Since CT scanning cannot capture intervertebral discs, Solidworks software was subsequently utilized to import the STL files and model the intervertebral discs, while also performing edge smoothing operations on the models, as shown in Fig. 1(c). The hybrid performance system for dynamic spine stabilization was modeled using Solidworks software. To optimize computational analysis time, the bone screws in the spinal dynamic stabilization system were partially simplified, as shown in Fig. 2(a). The simplification focused on the screw threads and the rigid rod fixation mechanism. The simplified dynamic stabilization system and bone screw models were then virtually implanted into the spinal model, as depicted in Figs. 2(b) and 2(c) for the spinal model created in Mimics software and the intervertebral disc created in Solidworks software. In this study, we used the commercial software ANSYS Workbench for analysis. In the material property settings, the Poisson's ratio and Young's modulus of the vertebral body were set to 0.3 and 12 GPa, while those of the intervertebral disc were set to 0.45 and 40 MPa, respectively.^(11,12) In this study, we focused on analyzing and exploring the degree of degeneration of the intervertebral disc. Therefore, the Young's moduli of the intervertebral disc were reduced to 50 and 80% to simulate severe degeneration and moderate degeneration, respectively.⁽¹²⁾

3. Simulation Results and Discussion

In the HPS, the dynamic spring segments were simulated using the longitudinal spring element created in Workbench software. The dynamic spring in HPS had already undergone static tensile and compression tests using a materials testing machine, and the stiffness obtained from these tests was 57 N/mm. The tensile and compression curves were input into the spring stiffness settings of the established longitudinal spring. The group analyzed and discussed the spring stiffness by reducing and increasing it by 50%, as well as the spring stiffness of commercially available spinal dynamic stabilization systems. Therefore, in the finite element model, the spring stiffnesses K1, K2, and K3 were set to 28, 57, and 85 N/mm, respectively. The spinal finite element model was subjected to three distinct motions: lateral bending, extension,

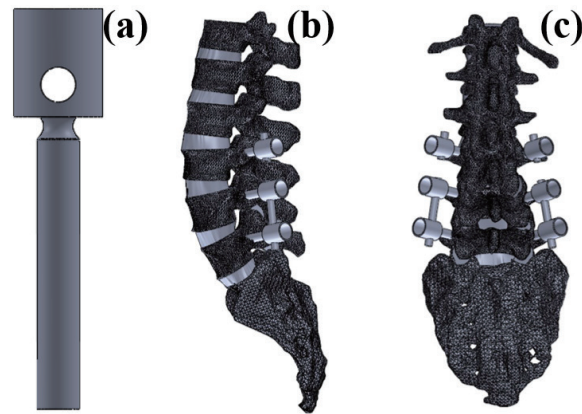


Fig. 2. (Color online) (a) Simplified bone screw model (diameter: 5.5 mm) and (b) lateral and (c) posterior views of the spinal model with HPS implantation.

and flexion. Each motion was applied with a torque of 7.50 N/m, combined with an axial compression force of 500 N to simulate upper body weight. We examined two levels of intervertebral disc degeneration: moderate and severe. For reference, a normal intervertebral disc was characterized by a Young's modulus of 40.0 MPa and a Poisson's ratio of 0.450. Prior to conducting the main analyses, a convergence test was performed on the moderate disc degeneration group (Disc E = 32 MPa) during flexion motion. The convergence analysis employed mesh sizes ranging from 1.5 to 2.5 mm, specifically testing at 1.50, 1.60, 1.70, 1.80, 1.90, 2.00, and 2.50 mm. The finite element model achieved both stress and displacement convergence at a mesh size of 1.80 mm, with numerical errors remaining within 1.0%.

On the basis of these results, a model with a total element count of 919139 was adopted for subsequent analyses, as demonstrated in Fig. 3. The finite element analysis conducted in this study provides valuable insight into the effects of varying coupler stiffness and disc degeneration on spinal mechanics. The sensitivity of adjacent segment stress and vertebral mobility to changes in spring stiffness highlights the importance of accurately modeling these parameters to predict postsurgical outcomes. The successful convergence test further ensures the robustness of the model, minimizing potential errors in simulation results. By considering different levels of intervertebral disc degeneration, we simulated realistic conditions that the spine may experience in both healthy and degenerative states. These findings may aid in optimizing spinal implant design and provide a better understanding of how mechanical changes affect spinal health over time.

In this study, we conducted axial loading tests including flexion, extension, and lateral bending on the specimen, with axial loads applied through steel wires, pulleys, and weights on both sides. The applied axial pressures (500 and 250 N per side) and bending moment (7.50 Nm) were designed to simulate physiological spinal loads in the human body. The axial pressure (500 N) and bending moment (7.5 Nm) applied in this experiment were based on literature reports, simulating the physiological loads exerted on the spine by the human body.^(13,14) For vertebral kinematics, a three-dimensional motion analysis system was employed to capture the relative motion of each vertebral segment, including displacements in three directions and

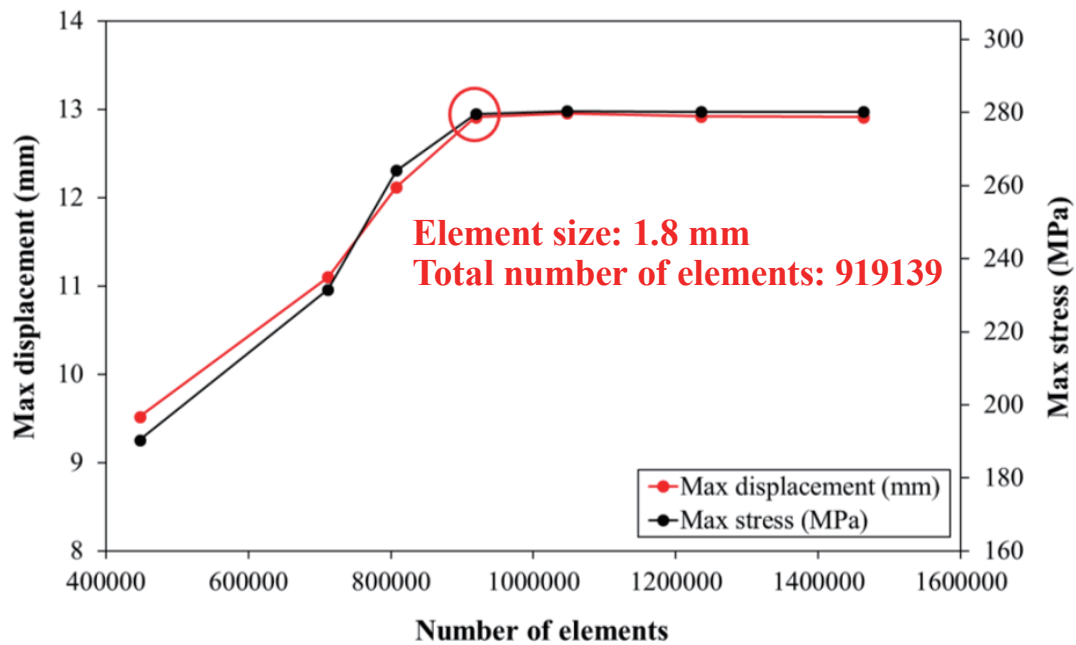


Fig. 3. (Color online) Convergence analysis of spinal finite element model.

rotations about the x -, y -, and z -axes. The flexion, extension, and lateral bending movements were applied at a rate of 0.005 Hz. Throughout the experiment, continuous recordings were made of the moments, intradiscal pressure, and three-dimensional motion data of each vertebral segment. Each movement was repeated three times, and the average of these three measurements was used as the final result. These experimental results were then compared with the finite element model analysis to verify the model's accuracy.

Figure 4 shows a comparison of the results of finite element model analysis with experimental measurements of spinal segment mobility. As shown in Fig. 4(a), when a 7.50 N/m flexion torque was applied, the analysis results from the finite element model were slightly lower than the experimental values. The largest discrepancy in segment mobility was observed at the T12 vertebra (12.7° vs 13.6°), with an error of 6.71%. Figure 4(b) shows that under extension moments, the model results were slightly higher than the experimental measurements, with the T12 vertebra again exhibiting the largest error (3.41° vs 3.22°), yielding a 6.29% discrepancy. In the lateral bending case, as shown in Fig. 4(c), the L1 vertebra showed the largest error (1.22° vs 1.11°), with an error of 8.29%. The errors remained below 8.29%, which is acceptable for engineering applications. Despite the large biological variation and the nonlinear characteristics of many tissues, the model demonstrates acceptable accuracy for biomechanical studies and can be further applied to investigate the impact of HPS coupler design parameters on vertebral mobility and disc stress.

These findings merit deeper consideration from both theoretical and practical perspectives. The consistency of error margins remaining below 8.29% across all loading conditions is particularly noteworthy, especially given the inherent complexities of biological systems. This

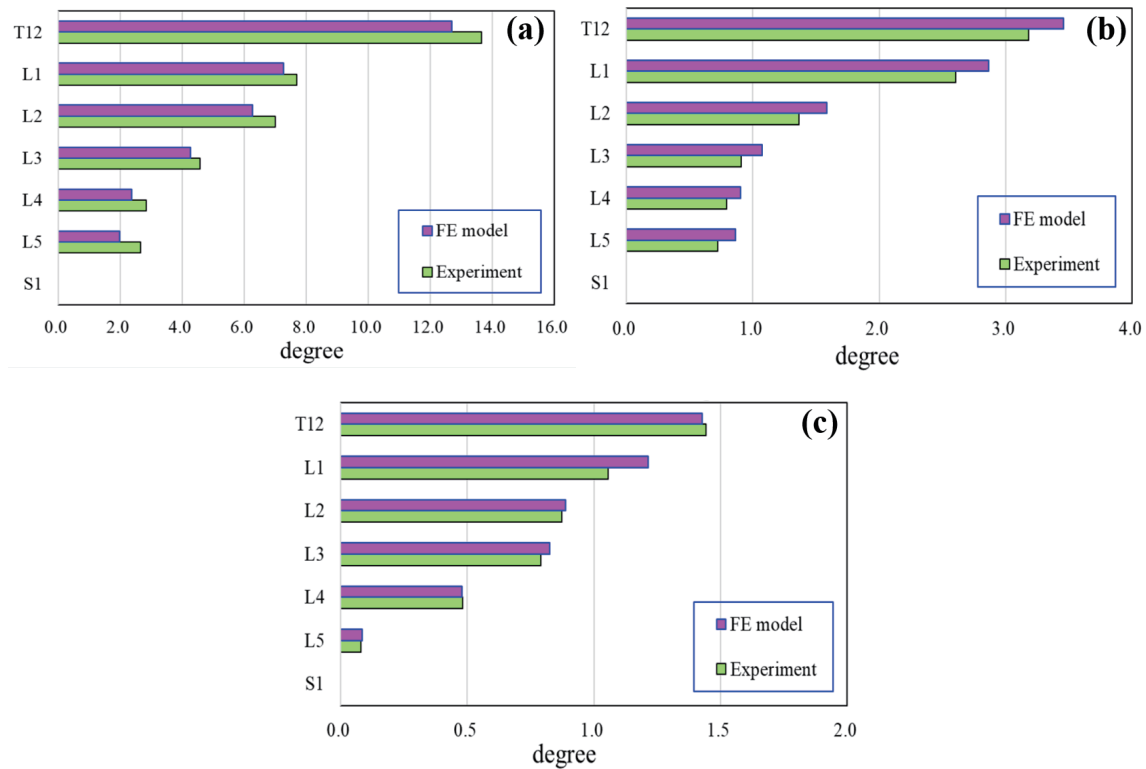


Fig. 4. (Color online) Comparison of results of finite element model analysis with experimental measurements in vertebral range of motion: (a) flexion moment, (b) extension moment, and (c) lateral bending moment.

level of accuracy is remarkable considering the significant challenges in modeling biological tissues, which include material property variations among individuals, age-dependent characteristics, and the complex nonlinear behavior of spinal components. The model's ability to maintain reasonable accuracy across different loading scenarios suggests its robust formulation and careful consideration of key biomechanical parameters. Furthermore, the systematic pattern of slight underestimation in flexion and overestimation in extension can provide valuable insights for future model refinements. The demonstrated accuracy makes this model particularly valuable for investigating HPS coupler design parameters and their effects on vertebral mobility and disc stress, potentially leading to improved surgical outcomes and medical device designs. These results also establish a solid foundation for future research into more complex loading scenarios and patient-specific applications.

First, we explored the relationship between segmental mobility and the stiffness of three different coupler designs in a disc with moderate degeneration under forward flexion, extension, and lateral bending movements, as shown in Figs. 5(a) and 5(b). The analysis of the intervertebral disc with moderate degeneration ($E_m = 32.0$ MPa) showed that as the stiffness of the HPS system increases, the mobility of the L3 segment decreases. As shown in Fig. 5(a), during forward flexion, the L3 segment exhibited a 26.9% reduction in mobility when the HPS stiffness was 85.0 N/mm compared with 27.0 N/mm. A significant difference was also observed at the T12 segment, where the overall mobility decreased by 14.0%. Similarly, during extension movements

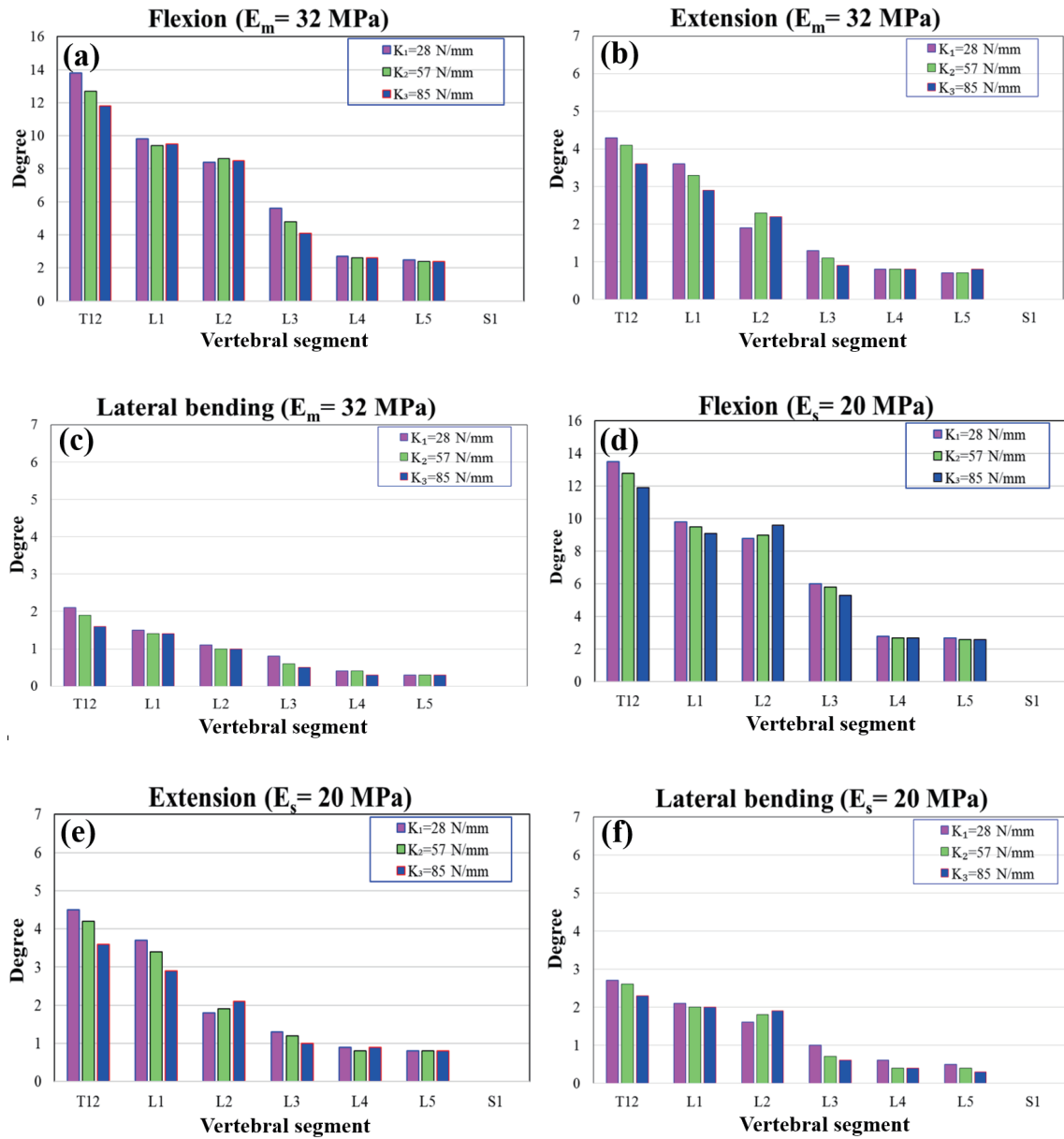


Fig. 5. (Color online) Three different coupler stiffness levels and the mobility of each segment of the intervertebral disc under different motions—for moderate degeneration: (a) forward flexion, (b) extension, and for severe degeneration: (c) lateral bending, (d) forward flexion, (e) extension, and (f) lateral bending.

in Fig. 5(b), the mobilities of the L3 and T12 segments decreased by 30.8 and 16.1%, respectively. In this section, we further explore the effects of HPS systems on intervertebral discs under moderate and severe degeneration conditions, considering three different coupler stiffness designs under forward flexion, extension, and lateral bending movements. In the moderate degeneration model ($E_m = 32.0$ MPa), the analysis showed that as the HPS stiffness increases, the mobility at the L3 segment decreases. In the forward flexion case shown in Fig. 5(a), the mobility

at the L3 segment decreased by 26.9% when the HPS stiffness was 85.0 N/mm compared with 27.0 N/mm, with the T12 segment also showing a notable reduction of 14.0%. In the extension group in Fig. 5(b), similar reductions were observed, with the mobilities of the L3 and T12 segments decreasing by 30.8 and 16.1%, respectively.

Figure 5(c) shows that under lateral bending, the mobility of each vertebral segment is significantly lower than forward flexion and extension. This is due to the more upright joint surfaces of the lumbar vertebrae than those in the cervical or thoracic spine, which restrict lateral bending motion. The analysis also revealed that the HPS system's coupler further limits the spinal mobility during lateral bending. Figures 5(d)–5(f) illustrate the mobility analysis of each vertebral segment under the effects of forward flexion, extension, and lateral bending torques in a severely degenerated disc ($E_m = 32.0$ MPa), using three different coupler stiffness designs. In Fig. 5(d), during forward flexion, the mobility at the adjacent segment (L2) is higher than in the moderate degeneration case. At HPS stiffnesses of 28.0, 57.0, and 85.0 N/mm, the mobility increased by 6.8, 21.2, and 29.1%, respectively. In the lateral bending movement, the adjacent segment (L2) also showed an increase in mobility by 25.2, 16.8, and 20.1%, respectively. However, during extension, no significant increase in mobility was observed, as shown in Figs. 5(d)–5(f). In these results, the adjacent segment (L3) also exhibited a lower mobility as the HPS stiffness increased. For lateral bending, the differences in segmental mobility produced by the three coupler designs were not significant. The results of these analyses highlight the important effect of HPS system stiffness on segmental mobility, particularly at the L3 segment.

As stiffness increases, mobility decreases, which suggests that the stiffness of the HPS system can play a critical role in controlling spinal movement, especially in cases of moderate degeneration. This effect is consistent across different motions (forward flexion, extension, and lateral bending) and is more pronounced at lower segments such as L3. Interestingly, the response in the severe degeneration model ($E_m = 32.0$ MPa) revealed some variability in the results, especially with lateral bending and forward flexion, where adjacent segments exhibited mobility that increased with HPS stiffness. This could suggest that in severely degenerated discs, the surrounding structures compensate for the increased stiffness of the HPS system. The lack of significant mobility increase during extension in the severely degenerated model may imply that the extension movement is less sensitive to the changes in the stiffness of the HPS system in this scenario. In future research, we can further investigate the underlying mechanisms that govern the differential mobility responses observed, particularly in severe degeneration cases. Additionally, evaluating the long-term effects of varying HPS stiffness in both moderate and severe degeneration conditions will be critical in understanding the implications for clinical applications and patient outcomes.

4. Conclusions

In this research, we investigated intervertebral disc degeneration, focusing on moderate and severe conditions, while establishing baseline characteristics for normal discs with a Young's modulus of 40.0 MPa and a Poisson's ratio of 0.450. Through a comprehensive convergence analysis utilizing mesh sizes between 1.50 and 2.50 mm, the finite element model demonstrated

optimal performance at a mesh size of 1.80 mm, maintaining numerical errors within 1%. This led to the implementation of a model comprising 919139 elements for subsequent analytical work. From both theoretical and practical standpoints, remarkable findings were obtained in this study, particularly in maintaining error margins consistently below 8.29% across various loading conditions—a significant achievement given the complexity inherent in biological systems. We revealed an inverse relationship between stiffness and mobility, highlighting how the HPS system's stiffness significantly affects spinal movement, especially in cases of moderate degeneration. This relationship manifested consistently across different types of motion, including forward flexion, extension, and lateral bending, with particularly pronounced effects observed in lower segments such as L3. The findings underscore the intricate interplay between mechanical properties and spinal functionality, providing valuable insights for both clinical applications and future research directions in spinal biomechanics. This understanding of the relationship between stiffness and mobility can be instrumental in developing more effective treatments for intervertebral disc degeneration.

Acknowledgments

This research was supported by the Marine Culture & Tourism Integration of Fujian Higher Educational Applied Liberal Arts Research Center under Project Nos. HYWL20240204, NSTC 113-2622-E-390-001, and NSTC 113-2221-E-390-011.

References

- 1 M. Nordin and V. H. Frankel: *Basic Biomechanics of the Musculoskeletal System*, (Lipincott Williams & Wilkins, Philadelphia, 2012) 4th ed.
- 2 H. J. Wilke, F. Heuer, and H. Schmidt: *Spine* **34** (2009) 255.
- 3 W. R. Sears, A. C. Solterbeck, and J. A. Kos: *Eur. Spine J.* **30** (2021) 181.
- 4 A. Angelini, R. Baracco, A. Procura, U. Nena, and P. Ruggieri: *Diagnostics* **11** (2021) 1891.
- 5 U. Chamoli, A. D. Diwan, and N. Tsafnat: *J. Biomed. Mater. Res. Part A* **102** (2014) 3324.
- 6 M. J. H. Dijk, N. T. A. Smorenburg, Y. F. Heerkens, J. Mollema, H. Kiers, M. W. G. Nijhuis-Sanden, and B. Visser: *Gait Posture* **76** (2020) 346.
- 7 X. Ren, S. Wang, D. Xiong, G. Tian, B. Lan, W. Yang, and W. Deng: *Chem. Eng. J.* **485** (2024) 149817.
- 8 S. T. Tsai, C. Y. Lin, S. M. Wu, C. Y. Chang, and C. F. Yang: *Microsyst. Technol.* **24** (2018) 4017.
- 9 D. S. Shin, K. Lee, and D. Kim: *Comput.-Aided Des.* **39** (2007) 559.
- 10 D. U. Erbulut, I. Zafarparandeh, A. F. Ozer, and V. K. Goel: *Adv. Orthopedics* **2013** (2013) 451956.
- 11 M. Xu, J. Yang, L. Isador, and H. Ram: *Med. Eng. Phys.* **63** (2019) 26.
- 12 H. Yang, M. G. Jekir, M. W. Davis, and T. M. Keaveny: *J. Biomech.* **49** (2016) 1134.
- 13 T. M. Stoll, G. Dubois, and O. Schwarzenbach: *Eur. Spine J. Suppl.* **2** (2002) S170.
- 14 K. J. Schnake, S. Schaeren, and B. Jeanneret: *Spine* **31** (2006) 442.